



An Investigation Into the Influence of Viscosity on Gear Churning Losses by Considering the Effective Immersion Depth

Joseph F. Shore, Anant S. Kolekar, Ning Ren & Amir Kadiric

To cite this article: Joseph F. Shore, Anant S. Kolekar, Ning Ren & Amir Kadiric (2023): An Investigation Into the Influence of Viscosity on Gear Churning Losses by Considering the Effective Immersion Depth, Tribology Transactions, DOI: [10.1080/10402004.2023.2247041](https://doi.org/10.1080/10402004.2023.2247041)

To link to this article: <https://doi.org/10.1080/10402004.2023.2247041>



© 2023 The Author(s). Published with license by Taylor & Francis Group, LLC.



[View supplementary material](#)



Published online: 05 Sep 2023.



[Submit your article to this journal](#)



Article views: 105



[View related articles](#)



[View Crossmark data](#)

An Investigation Into the Influence of Viscosity on Gear Churning Losses by Considering the Effective Immersion Depth

Joseph F. Shore^a , Anant S. Kolekar^b, Ning Ren^b, and Amir Kadiric^a 

^aTribology Group, Department of Mechanical Engineering, Imperial College London, London, United Kingdom; ^bVGP Holdings, LLC (Valvoline), Lexington, Kentucky, USA

ABSTRACT

We present an experimental investigation into the influence of oil viscosity on gear churning losses in splash-lubricated transmission systems. The inertia rundown method was used to perform tests on a single gear within a cylindrical housing with several oils of different viscosities at several immersion depths. A complex and nonmonotonic relationship between churning torque and viscosity was observed that was highly influenced by the rotational speed, with higher viscosity oils resulting in lower churning torque at higher speeds in some cases. This was attributed to a reduction in effective immersion depth due to oil being centrifugally distributed around the casing by the rotating gear, an effect that was observed to be more pronounced with higher viscosity oils. An effective immersion depth parameter, dependent on the rotational speed of the gear and the lubricant viscosity, was defined to account for this phenomenon. Gear churning losses could be better predicted using an existing empirical model when this parameter was used instead of the nominal immersion depth as is usually done.

ARTICLE HISTORY

Received 22 February 2023
Accepted 8 August 2023

KEYWORDS

Gear churning losses;
transmission efficiency; drag
losses; lubricants

Introduction


Oil churning in dipped or splash-lubricated gear transmission systems accounts for a significant proportion of overall gearbox losses, particularly at high speeds (1). The magnitudes of these losses are difficult to predict, as they are dependent on the interaction of centrifugal, gravitational, hydrostatic, and Coriolis forces (2) and are affected by the properties of the oil and the system geometry (3). The mixing of oil and air caused by gear rotation results in a multiphase fluid environment and formation of droplets and bubbles as the oil is thrown around the gearbox, which further complicates the prediction of churning losses.

Selection of an appropriate gear immersion depth presents a complex optimization problem: Decreasing it may reduce gear churning losses, but since dip lubrication helps to regulate the gear temperature by the removal of heat by centrifugal fling-off of the lubricant from the teeth (4), this can cause an increased gear bulk temperature, a corresponding drop in oil film thickness in gear teeth contacts, and a subsequently increased risk of gear failure (5). Insufficient immersion depth may also mean that oil supply to the bearings is inadequate. Because of these potential reliability issues, possible improvements in efficiency through reduction in immersion depth have often been forgone in lieu of reliability, resulting in an intentional oversupply of oil in the

gearbox to reduce the risk of component failure (6). As the focus in the design of mechanical systems continues to shift in favor of improving efficiency, optimization of this parameter is becoming increasingly important.

While it is commonly assumed that increasing oil viscosity leads to greater gear churning losses, which is one of the driving forces behind current trends among original equipment manufacturers (OEMs) to push for lower and lower viscosity fluids, the relationship between oil viscosity and churning power losses is a complex one and it may not be the case that this relationship is strictly monotonic; both Leprince et al. (7) and Kolekar et al. (1) observed experimentally that the use of low-viscosity lubricants led to increased churning losses under some conditions. One complexity is the influence of viscosity on the dynamic equilibrium in the oil surface profile, which Chen and Matsumoto (8) described as the steady-state oil surface profile (SOSP). By using a rotatable test rig with several different casing geometries, they demonstrated that there were significant differences in SOSP when the gear case was differently oriented; the shape of the SOSP may result in local changes in the dynamic immersion depth of the gears and a corresponding change in churning torque. In a study on oil flow rates around a transmission in splash lubrication, Leprince et al. (4) investigated the distribution of oil around a casing

CONTACT Joseph F. Shore  joseph.shore15@imperial.ac.uk
Review led by S. Berkebile.

 Supplemental data for this article can be accessed online at <https://doi.org/10.1080/10402004.2023.2247041>

© 2023 The Author(s). Published with license by Taylor & Francis Group, LLC.

This is an Open Access article distributed under the terms of the Creative Commons Attribution License (<http://creativecommons.org/licenses/by/4.0/>), which permits unrestricted use, distribution, and reproduction in any medium, provided the original work is properly cited. The terms on which this article has been published allow the posting of the Accepted Manuscript in a repository by the author(s) or with their consent.

Nomenclature

b	gear facewidth [m]	T	total resistive torque [N · m]
C_{ch}	churning torque [N · m]	T_c	calibration torque [N · m]
C_m	dimensionless churning torque [—]	t	time [s]
D_p	gear reference diameter [m]	V_0	oil volume [m ³]
Fr	Froude number [—]	V_p	submerged gear volume [m ³]
g	gravitational acceleration (9.8 m · s ⁻²)	z	number of gear teeth [—]
H	casing fill level [m]	ν	kinematic viscosity [m ² · s ⁻¹]
h	immersion depth [m]	ρ	oil density [kg · m ⁻³]
h_{eff}	effective immersion depth [m]	ϕ	minimum oil depth fraction [—]
m_n	gear module [m]	ω, Ω	rotational speed [rad · s ⁻¹ , rev · min ⁻¹]
Re	Reynolds number [—]	X	dimensionless group [—]
R_p	gear reference radius [m]		
S_m	submerged gear surface area [m ²]		

by a rotating gear by measuring the flow rates of oil projected to different locations of the casing wall at varying speeds. To do this, the flow rate of oil into a movable aperture on the casing wall was measured. They noted that at low rotational speeds, a significant quantity of oil is located at the gear periphery and moves with it, leading to the expulsion of a significant amount of oil to the walls near the gear. At higher rotational speeds centrifugal forces become predominant, resulting in no overall bulk fluid motion. The flow rates were shown to be highly viscosity dependent at both low and high speeds, with reduced flow rates observed at lower viscosities. At very low speeds, the flow rate to the aperture on the casing wall reduced to zero. At high speeds, the centrifugal distribution of oil up the sides of the casing may lead to a localized reduction in effective immersion depth of the gears, resulting in a reduction in churning torque. This effect may be less pronounced with lower viscosity oils, as they more readily flow back to the sump under gravity (1). Kolekar et al. (1) demonstrated the influence of windage on the oil disposition within the casing, with the magnitude of churning losses increasing by a factor of up to 4.5 when air was evacuated from it. Increased air pressure also reduced churning losses with a high viscosity oil under some conditions. The effects of the changing SOSP may lead to complex relationships between speed and churning torque, with centrifugal effects playing a crucial role. Stavtyskiy et al. (2) found that this relationship approximated a cubic parabola up to a certain speed, beyond which there is a slight reduction in hydrodynamic drag attributed to a reduction of the volume of oil in the spaces between the gear teeth due to centrifugal effects.

Despite the complexity of the relationship between churning torque, viscosity and speed, in many existing models (9–13) the dependence of churning torque C_{ch} on rotational speed, ω , and kinematic viscosity, ν , is expressed through a simple general relationship of the type shown in Eq. [1],

$$C_{ch} \propto \nu^{\lambda_1} \omega^{\lambda_2} \quad [1]$$

where λ_1 and λ_2 are constants, the exact values of which depend on the regime in which the gear is operating.

In these models (9–13), the Vaschy–Buckingham Pi theorem is used to relate a nondimensionalized (ND) form of the churning torque, C_m , to dimensionless groups relating to the gear geometry, oil properties, and operating conditions in the form of Eq. [2],

$$C_m = \psi_1 \prod_{i=2}^n X_i^{\psi_i} \quad [2]$$

where ψ_{1-n} are constants determined by regression and X_i are ND groups.

How C_m is defined differs between researchers. Lauster and Boos (13) and Terekhov (12) relate C_{ch} to C_m using Eq. [3], while Boness (11) and Changenet et al. (9, 10) use Eq. [4]:

$$C_{ch} = \rho \omega^2 b R_p^4 C_m \quad [3]$$

$$C_{ch} = \frac{\rho}{2} \omega^2 S_m R_p^3 C_m \quad [4]$$

where ρ is the lubricant density, b is the gear facewidth, R_p is the gear pitch radius, and S_m is the submerged gear surface area.

Lauster and Boos (13) described ND churning torque using a single expression, while Terekhov (12) described it with three, with the expression used being dependent on the Reynolds and Froude numbers, defined by Eqs. [5] and [6], respectively:

$$Re = \frac{\omega R_p^2}{\nu} \quad [5]$$

$$Fr = \frac{\omega^2 R_p}{g} \quad [6]$$

where g is gravitational acceleration (9.8 m · s⁻²).

Similarly, Boness (11) proposed a model with three regimes. However, in this model the magnitude of ND churning torque is determined by the Reynolds number exclusively. In this model the characteristic length used in the definition of the Reynolds number is the length of the chord at the nominal immersion depth, rather than R_p . Changenet et al. (9, 14) proposed a two-regime model, defining a critical Reynolds number Re_c , defined by $Re_c =$

$\omega R_p b / \nu$, to determine whether the gear operates in a high- or low-speed regime. In a later paper (10), they introduced an additional parameter γ , analogous to the centrifugal acceleration and defined by $\gamma = \omega^2 (R_p b m_n)^{1/3}$, where m_n is the gear module. This further separated the flow into four regimes. In the transition regions between the regimes, linear interpolation between the formulas is used.

There are large differences between researchers when it comes to the values of the exponents in Eq. [1]. The discrepancies are most stark when comparing the predicted influence of viscosity on churning torque. The model proposed by Boness (11) suggests that at high Reynolds numbers viscosity is at its most influential on churning torque, with $\lambda_1 = 2$, in contradiction to the models proposed by Changenet et al. (9, 10), which suggest churning torque is insensitive to viscosity at high Re ($\lambda_1 = 0$). The discrepancies in the value of churning torque predicted using different models is often significant. Luke and Olver (15) performed a comparative study of the formulas proposed by Boness (11) and Terekhov (16), finding that the magnitude of the predicted losses differed by a factor of 50 in some cases. The lack of consistency between the models in the literature may at least in part be due to overfitting of the empirical models to specific sets of experimental results, limiting the universal applicability of the models.

The nonmonotonic relationship between churning torque, speed, and viscosity may be captured by some of these models; Boness's (11) formulas describe a transition region between laminar flow and turbulence where churning torque decreases with increasing Reynolds number, with $\lambda_1 = -0.33$, corresponding with increasing viscosity. In the models such as those proposed by Changenet et al. (9, 10, 14) and by Terekhov (12), where λ_1 is either positive or zero depending on the regime in which the gears operate, predicted churning torque may not increase monotonically with viscosity, as the regime in which the gears operate is determined by the Reynolds number, which itself is viscosity dependent. As a result, there may be a local decrease in predicted losses with increasing viscosity in the transition between the formulas describing the different flow regimes in some cases. However, there appears to be little agreement on where these transitions occur.

Due to the influence of the oil surface profile on churning losses, it may be reasoned that consideration of an "effective" immersion depth, which better reflects the oil distribution in the gearbox during actual operation, may be a key factor in better describing the complex relationship between gear churning torque and oil viscosity and should be included in any model able to accurately predict gear churning losses. Quiban et al. (17) considered the effective immersion depth in an experimental investigation into churning losses in spiral bevel gears at high speed by measuring the resistive torque exerted on a single gear rotating in a sump. They modified the formula for churning in spiral bevel gears proposed by Laruelle et al. (18) by defining a "dynamic" ND immersion depth, a function of the static immersion depth. This value could be substituted into this model in place of the static immersion depth to better predict churning losses at high speeds, accounting for the reduction in effective immersion depth. The criteria for use of

the static or dynamic value was based on a second Froude number, defined as $Fr^* = \omega R_0 / \sqrt{gh}$, where R_0 is the outside gear radius. At low speeds, where $Fr^* < 25$, the static value was used, while at high speeds, where $Fr^* > 50$, the dynamic value was substituted. When $25 < Fr^* < 50$, a linear transition between the static and dynamic values was implemented. While this approach appeared to significantly improve the model predictions, only a narrow range of viscosities was tested in this study and the transition between static and dynamic was solely defined by Fr^* ; the influence of viscous forces on SOSF observed by Chen and Matsumoto (8) is thus not adequately accounted for. In a series of studies on gear churning losses in planetary gears, Boni et al. (19, 20) considered the influence of oil surface profile on losses by modifying the model described by Changenet et al. (10) to account for the formation of an "oil ring" around the circumference of the cylindrical housing, adjusting the submerged surface area parameter to that which would be expected when this ring is formed. The criterion for whether this ring was formed was based on a relationship between the Reynolds and Froude numbers, thereby considering both speed and viscosity. Crucially, they observed that a lower viscosity fluid would not necessarily lead to lower churning losses, due to the effects on the oil surface profile.

Clearly, there are significant disagreements between researchers when it comes to the influence of oil viscosity on gear churning losses. Due to the dynamic nature of the system, the nominal immersion depth appears to be insufficient to describe the distribution of oil within the casing. Instead, it seems that the "effective" immersion depth, accounting for the change in oil surface profile as the gear rotates, is a key parameter in understanding the link between viscosity and churning losses. Up to now, attempts to explore the importance of the effective immersion depth and its use in empirical models for prediction of churning have been limited. This study attempts to improve our understanding of the relationship between oil viscosity and gear churning losses by first conducting a set of systematic experiments to measure churning torque over a wide range of viscosities and gear rotational speeds, and then explaining the observed trends by considering the effective oil immersion depth. The latter includes simple modification to existing churning loss models to include an effective immersion depth parameter using nonlinear regression. The findings can help in selecting appropriate oil viscosity for a given gear application to minimize gear churning losses.

Experimental methods

Churning losses have been determined experimentally using the inertia rundown rig described in reference (1). The rig and its main components are shown in Fig. 1.

This rig consists of an electric motor with a step-up belt drive, which drives the test gear in its housing. The gear shaft is coupled to the driven pulley shaft with a manually disconnected dog clutch. The nylon test spur gear, with geometrical parameters listed in Table 1, is mounted on the gear shaft and rotates in the oil sump. The gear is situated

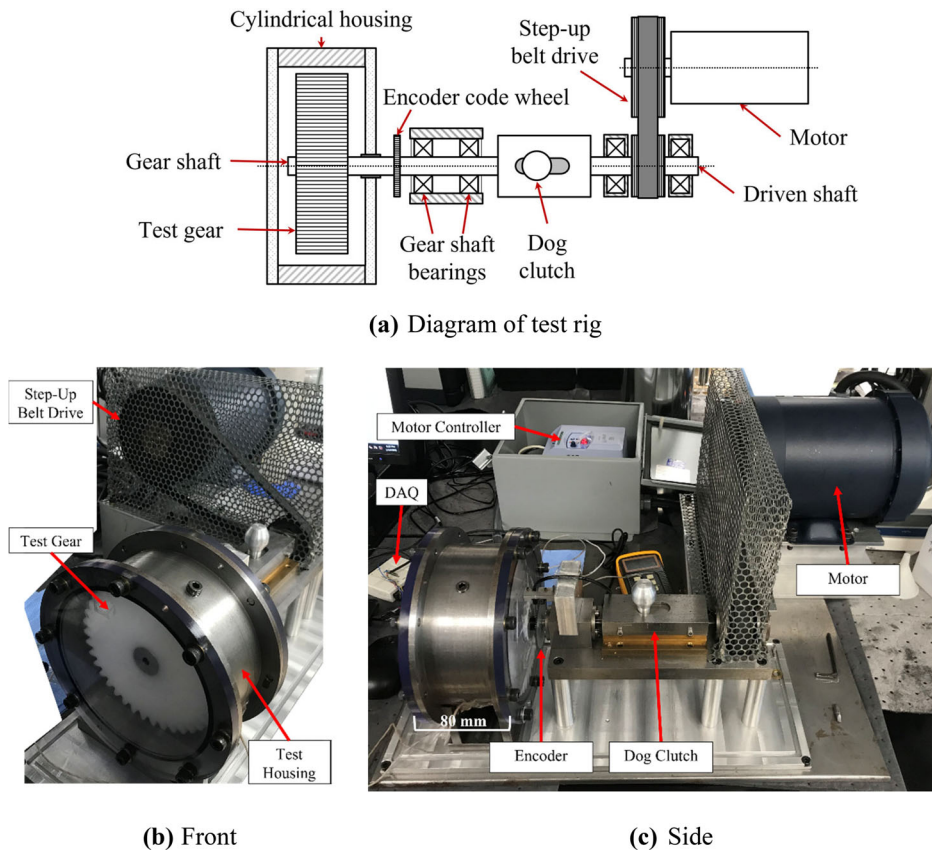


Figure 1. Gear churning inertia rundown test rig: (a) schematic diagram of the rig, (b) photograph of the front of the rig showing test gear in its housing, and (c) photograph of the side of the rig.

Table 1. Geometry of the test gear.

Module m_n	4 mm
Facewidth b	40 mm
Reference pressure angle α	20°
Number of teeth z	38

in a cylindrical housing which has an internal diameter of 168 mm and width of 80 mm. This is a relatively closely fitting housing chosen to mimic automotive transmissions (1). An optical encoder is mounted on the gear shaft to measure the rotational speed of the gear. As shown in Fig. 1a, the gear shaft is cantilevered on oil lubricated bearings that are external to the test housing. These bearings and their seals therefore do not interact with the oil in the gear housing. Sealed polycarbonate windows on either side of the gear housing were used to observe oil flow during the tests.

At the start of a test, the rig is run up to a specific speed. Once this speed is reached, the dog clutch is used to disconnect the gear shaft from the driven pulley shaft. The gear and gear shaft are then allowed to decelerate under their own inertia while the encoder measures their angular speed. The torque exerted on the gear by the lubricant can thereby be determined from the gear's deceleration by considering the inertia of the system. This method has the advantage of being able to quickly provide a sweep of data points over different speeds. As the rundown takes a relatively short period of time, typically less than 30 s, temperature changes in the oil sump are small within a single test, ensuring that churning torque is measured at an approximately constant viscosity for all speeds. In the tests

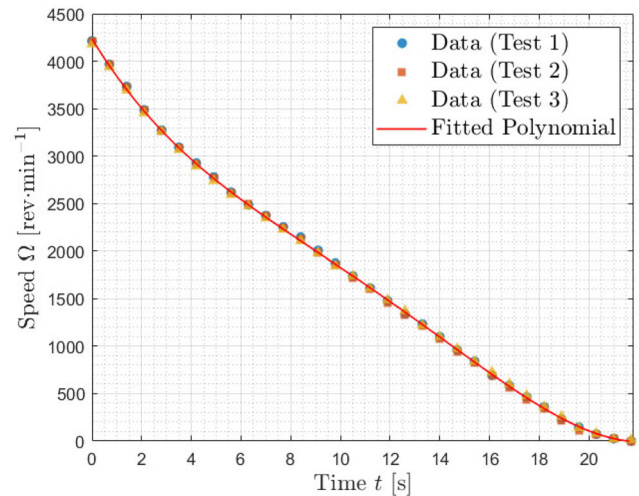


Figure 2. Examples of recorded gear rotational speed against time during gear deceleration for tests with a 75 cSt oil and oil level of 30 mm measured from the lowest point of the casing, with a fitted fifth-order polynomial function.

described in this paper, the average change in temperature during a complete set of rundown measurements was +0.1 °C, with the maximum change being less than +0.5 °C. The oil viscosity and density for each test were calculated at the average of the sump temperatures measured immediately before and immediately after each rundown. All tests were performed at room temperature of 20 °C.

Each rundown test was repeated three times and the repeatability was consistently excellent. To illustrate this, Fig. 2 shows results of three repeat measurements for this

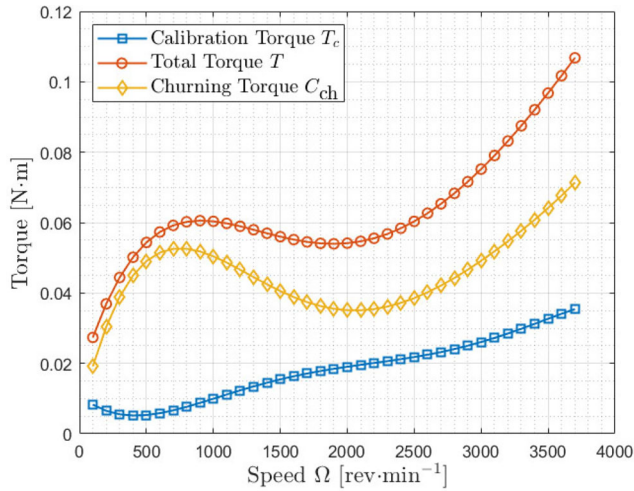


Figure 3. Example of measured total torque, T , and bearing and windage resistive torque (calibration torque), T_c , and hence calculated gear churning torque, C_{ch} .

Table 2. Kinematic viscosities and densities of the nine oils used in this study. All are PAO base stocks.

Oil number	$\nu_{40^\circ\text{C}}$ (cSt)	$\nu_{100^\circ\text{C}}$ (cSt)	$\nu_{20^\circ\text{C}}$ (cSt)	$\rho_{20^\circ\text{C}}$ ($\text{kg} \cdot \text{m}^{-3}$)
1	5.0	1.7	9	795.6
2	7.2	2.1	14	798.4
3	10.1	2.6	21	806.6
4	19.0	4.1	44	817.6
5	31.0	5.8	75	824.7
6	59.4	9.1	164	830.5
7	113.4	14.7	349	836.2
8	213.7	23.9	678	842.0
9	396.0	39.0	1273	847.7

specific case. Nevertheless, the average speed data from the three tests for each case were used in further analysis. To extract the resistive torque from the recorded speed data, first a fifth-order polynomial is fitted to this average speed data. An example of this is shown in Fig. 2. This polynomial is then differentiated with respect to time to obtain the deceleration of the gear as a fourth-order polynomial function. The resistive torque T is then calculated using Eq. [7]:

$$T = -I \frac{d\omega}{dt} \quad [7]$$

where ω is the rotational speed of the gear shaft in radians per second and I is the inertia of the system.

The value of T represents the total resistive torque, comprising that from the bearings and windage as well as that from gear churning. To isolate the gear churning torque, the rundown procedure was repeated in the absence of a lubricant sump to determine a calibration torque T_c , representing just the combined windage and bearing resistive torques. The churning torque C_{ch} can thereby be determined by subtracting the calibration torque T_c from the overall torque T (Eq. [8]). An example of measured T and T_c torques and subsequently calculated gear churning torque C_{ch} at different gear speeds is shown in Fig. 3.

$$C_{ch} = T - T_c \quad [8]$$

Calibration torque (i.e., parasitic bearing, seal, and windage torque) measurements were performed immediately

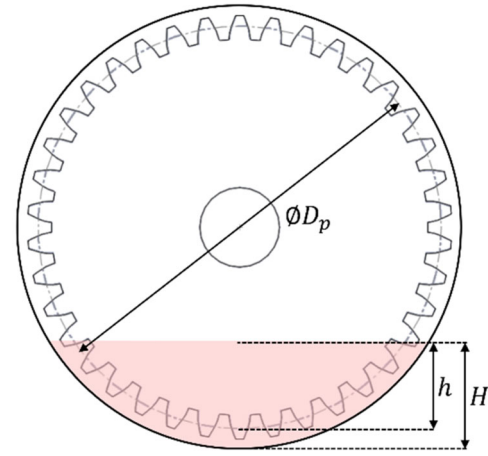


Figure 4. Definition of oil immersion depth h and oil fill level, H .

before and immediately after the gear churning tests; no appreciable discrepancy between these tests was observed beyond what may be expected from experimental variation. Nevertheless, the average of these measurements was used for calibration torque to account for any effects of bearing temperature increase on bearing losses.

A potential shortcoming of the inertia rundown method arises when the churning torque is small relative to the calibration torque. In these situations, the error incurred could be of the order of the calculated churning torque. Therefore, in cases where the churning torque accounted for less than 5% of the total torque, the data point was not included in the analyses presented in this paper.

Experimental conditions

Churning losses were measured with nine different viscosities of the same group IV/PAO base stocks. Different viscosities were obtained by blending PAO base stock of various viscosities in different volume ratios. The kinematic viscosities at 40 °C, 100 °C, and 20 °C and densities at 20 °C of these blends are listed in Table 2.

Each oil viscosity was tested at six immersion depths. The immersion depth of the gear h was defined as the height from the reference radius of the lowest tooth to the oil level in the gearbox, as shown in Fig. 4. Different immersion depths were achieved by filling the gearbox to different oil levels, H .

Transient effects

A potential shortcoming of the inertia rundown method is that it is inherently transient; the rotational speed of the gear is constantly changing. To make inferences relating to steady state conditions, we must assume that transient effects are negligible. To test this assumption, a series of tests was performed with different initial gear rotational speeds to vary the history of the oil surface profile. If these tests produce similar curves in the region where the speeds overlap, it may be reasonable to assume that any transient

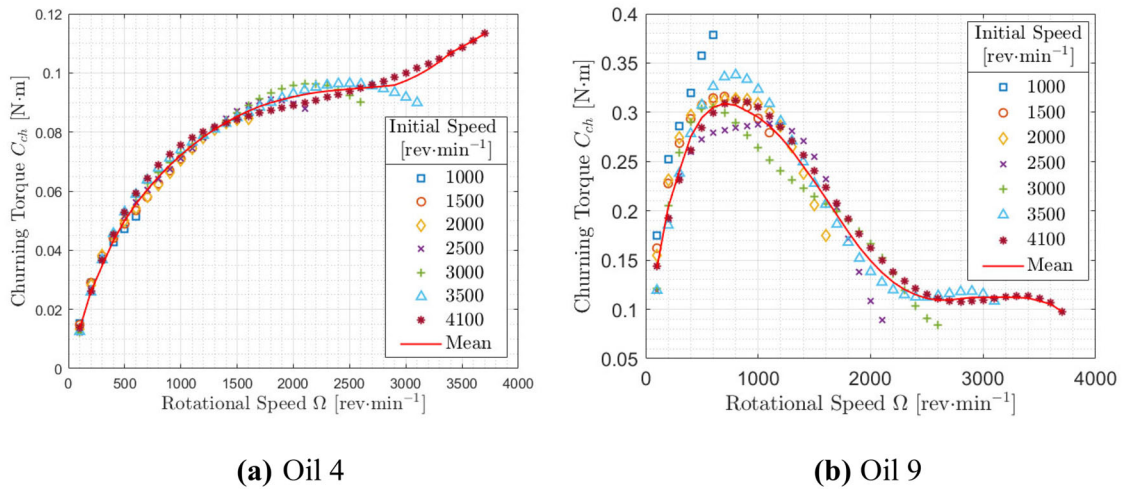


Figure 5. Churning torque measurements against gear rotational speed for varying initial speeds, $H = 40$ mm: (a) results for Oil 4 and (b) results for Oil 9 (see Table 2 for oil properties). Mean torque of all speeds is also shown.

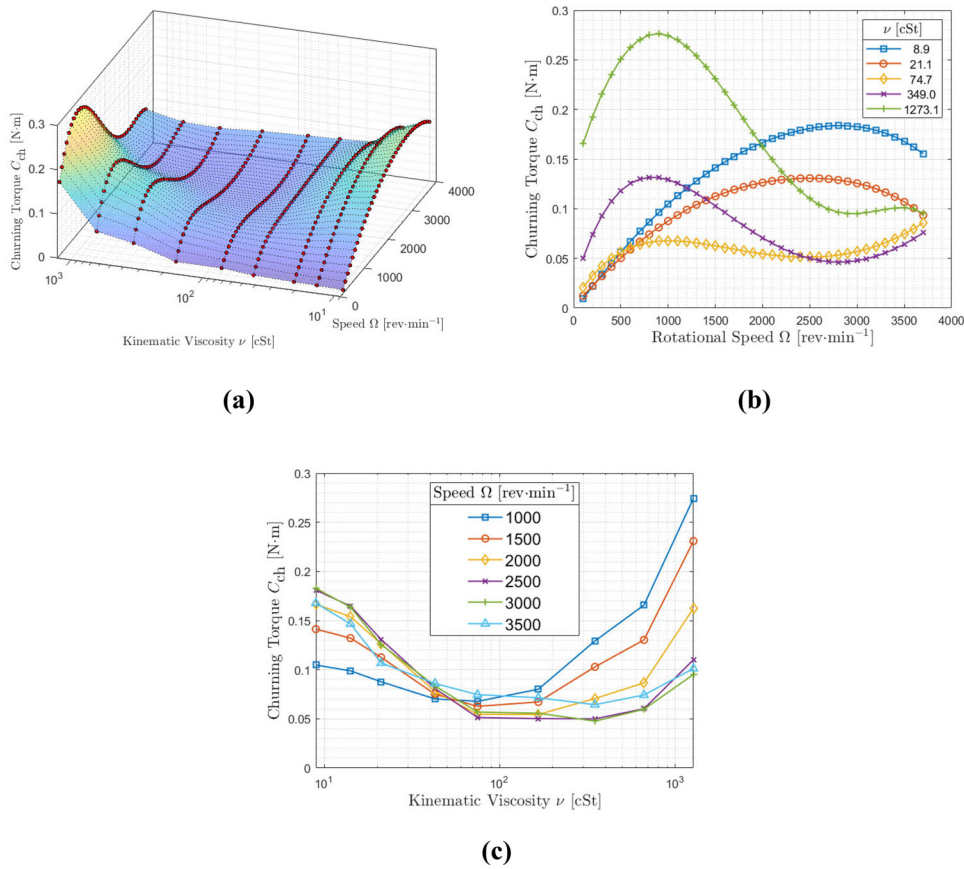


Figure 6. Measured gear churning torque against kinematic viscosity and rotational speed: (a) a surface plot of all results, (b) 2D plot of churning torque against rotational speed for a selection of viscosities, and (c) 2D plot of churning torque against kinematic viscosity for a selection of speeds. $H = 35$ mm.

effects are negligible. The results of two of these studies are shown in Fig. 5.

It is evident that the churning torque vs speed curves show the same trends and very similar absolute values regardless of the starting gear speed. This is particularly true for the lower viscosity Oil 4 shown in Fig. 5a. This suggests that it is acceptable to neglect transient effects in the inertia rundown measurements. Above around $3000 \text{ rev} \cdot \text{min}^{-1}$, there is a slight deviation in the curves. This may be because at these higher speeds, the deceleration of the gear is greater

than at lower speeds, and as such the inertia rundown measurements are less representative of steady-state conditions; however, the absolute difference in torque observed here is still low. It is apparent that the differences in the results for different starting speeds are more pronounced with the high viscosity Oil 9 shown in Fig. 5b than with the lower viscosity Oil 4 shown in Fig. 5a. This is likely due to the longer time it takes the high-viscosity fluid to reflow to its nominal level once pushed away by the rotating gear. Oil 9 was the highest viscosity tested here and its viscosity is much higher

than would be found in a commercial automotive gearbox. This therefore represents an extreme case, and the assumption of negligible transient effects is even more valid for lower viscosity fluids.

Results

Oil viscosity

Measured gear churning torque is plotted against oil viscosity and rotational speed in the surface plot of Fig. 6a. For clarity, Fig. 6b and Fig. 6c show the same data but as two-dimensional (2D) curves of torque versus speed for a selection of viscosities and of torque versus viscosity for a selection of speeds. The plots identify two different trends, one for the relatively high-viscosity oils (>100 cSt) and one for the lower viscosity oils. For high-viscosity oils, churning torque peaks at around $1000 \text{ rev} \cdot \text{min}^{-1}$; as speed increases, churning torque then decreases—for the highest viscosity oil the decrease reaches a plateau within the speed range tested, but for others, there appears to be yet another increase in torque toward the highest speeds tested here. In contrast, for oils with viscosities below 30 cSt, the churning torque continuously increases with speed up to about $3000 \text{ rev} \cdot \text{min}^{-1}$; some drop-off is then seen above this speed, but since the highest test speed was $3700 \text{ rev} \cdot \text{min}^{-1}$, the significance of this is unclear. The trend shown in Fig. 6c is more consistent: There appears to be an optimal viscosity, between 70 and 110 cSt for the present setup, where the churning torque is lowest for all gear speeds. At lower viscosities the churning torque can be up to three to four times higher than this minimum, and at highest viscosity tested, the churning torque is up to five times higher than the minimum. Interestingly, the churning torques near this optimal viscosity range are very similar (around 0.05 to $0.07 \text{ N} \cdot \text{m}$) for all gear speeds; therefore, in practical applications, the benefits of low churning torque can be realized for a wide range of gearbox speeds if an appropriate viscosity is chosen. In contrast, at viscosities higher or lower than this optimum range, speed has a significant influence on churning loss, as may be expected: namely, at low viscosities, higher speed

results in higher churning torques, while at high viscosities, the trend is reversed, with lower speeds producing highest churning torques.

Immersion depth

Figure 7a shows how the gear churning torque changes with nominal immersion depth, h , and speed in a three-dimensional (3D) surface plot. Figure 7b shows the same data in a 2D plot for clarity. A clear monotonic increase in churning torque with increasing nominal immersion depth was observed for all speeds. The rate of torque increasing with increasing immersion depth is also not significantly influenced by the speed, as can be seen in Fig. 7b. Similar results were observed with all other viscosities tested.

Effective immersion depth

In many previous studies (9–13) the Vaschy–Buckingham Pi theorem has been used to nondimensionalize several variables that influence gear churning losses. One common parameter that appears in existing gear churning models is the immersion depth h , normalized by the gear reference radius R_p (11–13) or diameter D_p (9, 10). This parameter represents the nominal dimensionless immersion depth of the gear. However, as the gear rotates, centrifugal effects and the disintegration of the oil sump lead to oil being deposited up the sides of the casing, thereby reducing the quantity of oil that can interact with the gear directly. This has the effect that the effective sump fill level during gear operation is less than nominal. Therefore, the “effective” immersion depth during gear rotation is less than the nominal immersion depth. The “effective immersion depth” is some fraction of the nominal immersion depth; the exact value of the fraction is dependent on rotational speed and oil viscosity. This general concept is illustrated in Fig. 8. Note that due to complex sump surface profile during running, this “effective immersion depth” may not correspond to any particular measured immersion depth at any specific location within the gearbox, but instead is a parameter defined to account

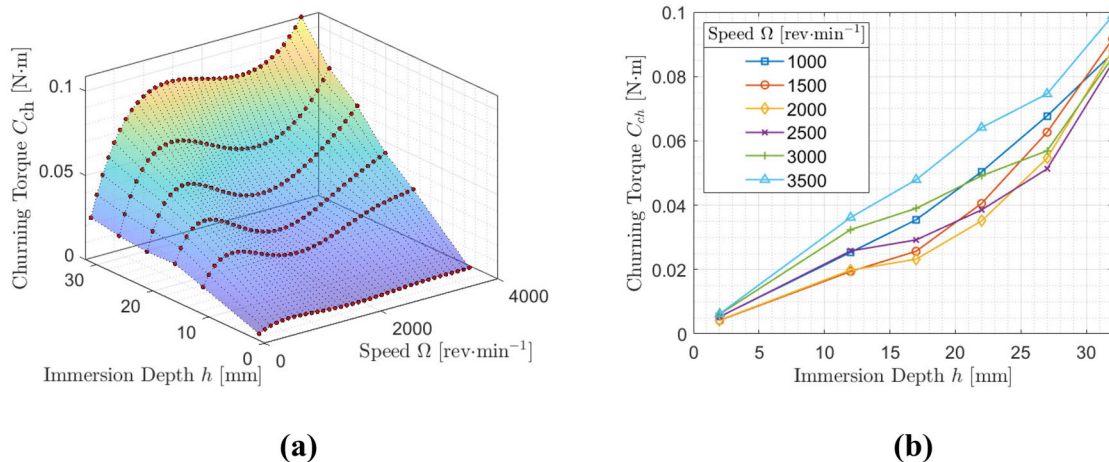


Figure 7. Measured churning torque at different immersion depths and gear rotational speeds: (a) a surface plot of all results, and (b) 2D plot of churning torque against immersion depth at a selection of speeds; Oil 5.

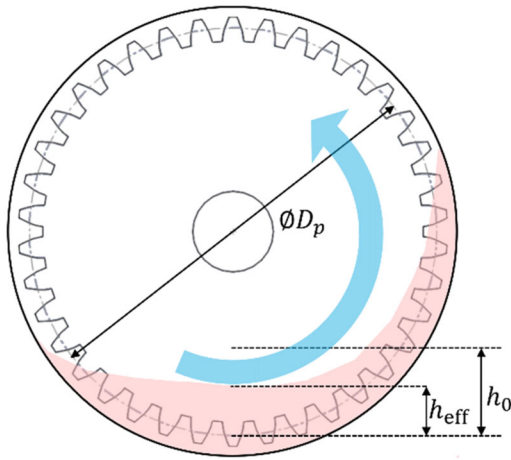


Figure 8. Illustration of nominal (h_0) and effective (h_{eff}) immersion depths.

for the observed effects. The effect is strongly influenced by the rotational speed of the gear and the viscosity of the lubricant and is clearly observable during churning experiments. To illustrate this, Fig. 9 shows a series of photos of the churning rig when running at different steady speeds for three different oil viscosities, ranging from a relatively low one of 9 cSt, via an intermediate 75 cSt, to a very high one 1273 cSt (all viscosities quoted at test temperature). In all cases, the oils are colored, purple, green, and red, so that the oil surface profile in the sump can be clearly seen. The first row of pictures is at 0 speed so shows the nominal immersion depth. As speed increases to $500 \text{ rev} \cdot \text{min}^{-1}$, then $1500 \text{ rev} \cdot \text{min}^{-1}$, $2500 \text{ rev} \cdot \text{min}^{-1}$, and finally $3500 \text{ rev} \cdot \text{min}^{-1}$, it is clearly seen that the level of oil in the sump reduces so that the effective immersion depth of the gear is less than the nominal depth. At the same time, the oil can be seen to be distributed around the casing. The effect is most prominent at the highest viscosity shown here (1273 cSt) where the effective immersion depth is minimal even at $500 \text{ rev} \cdot \text{min}^{-1}$.

The oil surface profile (SOSP) is complex when the gear is rotating, but the reduction in the effective immersion depth can be quantified for comparison purposes by measuring the effective immersion depth at the centre of the casing in the images of Fig. 9. The ratio of this approximate effective immersion depth h_{eff} at the center of the casing and the nominal immersion depth is plotted against the gear speed for the three test oils in Fig. 10. It is evident that for the highest viscosity and highest speed, the immersion depth measured here is only about 10% of the nominal depth. Even at $500 \text{ rev} \cdot \text{min}^{-1}$, the effective immersion depth has dropped to less than half of the nominal immersion depth. The effect is less prominent for lower viscosities but remains significant nevertheless, with reduction in immersion depth of 40% at the highest speed tested here.

Modification to an existing churning loss model

As only a single gear geometry was considered in this investigation, the accuracy of the predictions of any regressed fit may be limited to the geometry tested. Therefore, we have

limited the scope of this article to a modification to a well-established existing empirical model that may be used practically to better predict the nonmonotonic relationships observed.

It is evident from these results that both viscosity and gear speed influence the oil profile (SOSP) and hence the effective immersion depth. To capture this phenomenon numerically, an effective immersion depth parameter h_{eff} was defined using Eq. [9]:

$$h_{eff} = h_0 [\phi + (1 - \phi) \cdot \tanh \{a_1 Re^{a_2} Fr^{a_3} + a_4 Re^{a_5} Fr^{a_6}\}] \quad [9]$$

where a_{1-6} and ϕ are constants to be determined empirically.

It should be noted that the measurements shown in Fig. 10 were determined from the oil level at the center of the casing wall that is apparent in the photographs of Fig. 9. However, the SOSP is three-dimensional and non-axisymmetric. For example, the depth in the axial gap between the casing wall and the gear is likely to be lower than the values recorded at the wall. Therefore, the ratios shown in Fig. 10 may not be representative of the ratios calculated using Eq. [9], where h_{eff} is simply a fitting, rather than measured, parameter, which allows for the observed effects to be accounted for.

A hyperbolic tangent function of this form was selected so that, provided that the overall exponents of speed are negative (i.e., $a_2 + 2a_3 < 0$ and $a_5 + 2a_6 < 0$) and a_1 and a_4 are positive, the argument of the tanh function will tend toward zero as speed tends toward infinity. As a result, the effective immersion depth will tend toward ϕ , representing some minimum fraction of the nominal immersion depth. This value is expected to be dependent on the geometry of the gears and casing. For example, a different oil distribution may occur in a large casing than in one that is more closely conforming; the presence of baffles or deflectors may reduce the amount of oil being splashed around the casing and hence act to limit any reduction in effective immersion depth during operation.

As speed tends toward zero, provided that at least one of the Reynolds or Froude number exponents is negative, the argument of the function will tend toward infinity, and consequently the tanh function will tend toward unity. The effective dimensionless immersion depth will thereby tend toward the nominal dimensionless immersion depth.

This effective immersion depth parameter can now be substituted into the existing expressions for churning torque described by other authors to assess whether this would improve the ability of these models to capture some of the more complex trends illustrated by the experimental results shown here, in particular the decrease of churning torque with increasing speed for higher viscosities. This is done using the expression for churning torque produced by Lauster and Boos (13) (Eq. [10]) to produce the modified Eq. [11]:

$$C_m = 2.95 Re^{-0.15} Fr^{-0.7} \left(\frac{h}{R_p}\right)^{1.5} \left(\frac{b}{R_p}\right)^{-0.4} \left(\frac{V_p}{V_0}\right)^{-0.5} \quad [10]$$

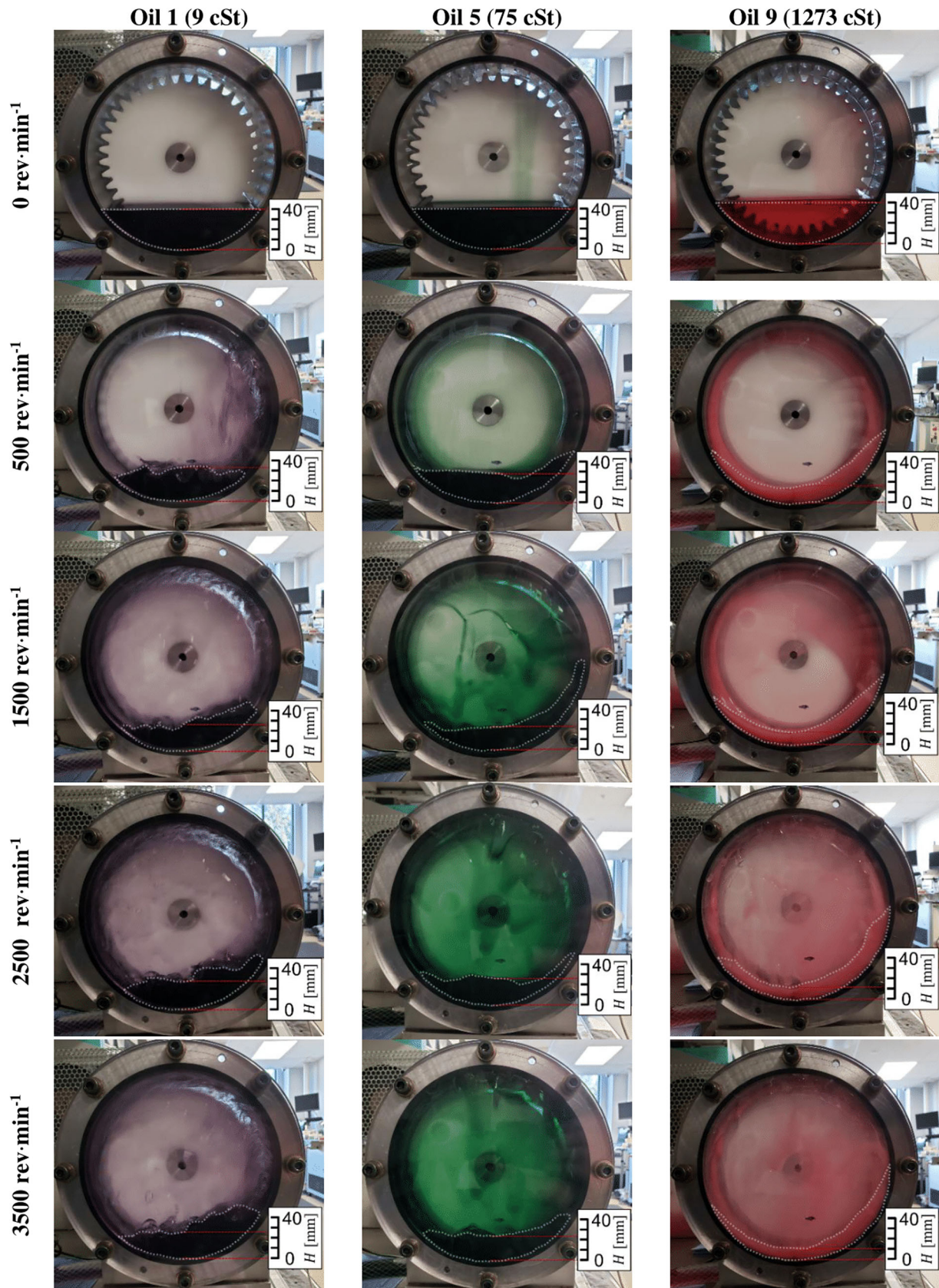


Figure 9. Photographs of the churning rig when running at different steady speeds (as indicated on the left) for three different oils: Oil 1, (left column, purple), Oil 5 (central column, green), and Oil 9 (right column, red). The nominal oil fill depth is 40 mm in all cases. The approximate SOSPs are indicated by dotted lines.

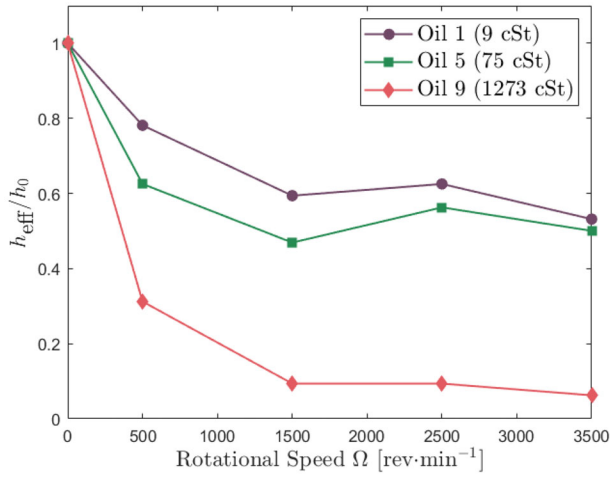


Figure 10. Plots of the ratio of “effective” immersion depth (as measured at the center of the casing using photos of Fig. 9) to nominal immersion depth, against gear speed. Three oils shown with viscosities at test temperature as indicated. Nominal oil fill level H of 40 mm.

Table 3. Regressed model parameters.

ϕ	a_1	a_2	a_3	a_4	a_5	a_6
0.24	4.99e-3	0.82	-0.65	5.78e3	-1.19	-0.62

$$C_m = 2.95Re^{-0.15}Fr^{-0.7} \left(\frac{h_{eff}}{R_p} \right)^{1.5} \left(\frac{b}{R_p} \right)^{-0.4} \left(\frac{V_p}{V_0} \right)^{-0.5} \quad [11]$$

where V_p/V_0 is the ratio of the immersed volume of the gear to the oil volume.

The regression procedure was also performed with the other aforementioned churning models (9–12) but these produced inferior fits compared to the modified Lauster and Boos model shown here and have been excluded for brevity.

Empirical fits

The model described by Eqs. [9] and [11] was fitted to the experimental data using a nonlinear regression routine. The regressed model constants as used in these equations are listed in Table 3.

Surface plots of churning power against kinematic viscosity and rotational speed for each immersion depth are shown in Fig. 11. This figure shows the model predictions matching the experimental data reasonably well over all the conditions tested. In particular, the local maxima observed at low speed with a high viscosity oil are captured. For clarity, Fig. 12 shows 2D plots of churning losses against speed for selected viscosities at $H = 40$ mm. The 95% confidence intervals (CI) for the model predictions are also shown. Here, it can be observed that the overall curvature of the plotted experimental data is reasonably well matched by the model predictions across the spectrum of viscosities tested.

The unmodified model (13) appears to predict churning losses accurately for the tests with low viscosity oils, as shown in Fig. 12a and 12b. This is understandable as the reduction in effective immersion depth is less pronounced in these cases. The modified model slightly underpredicts the losses in these cases but the predictions remain close to

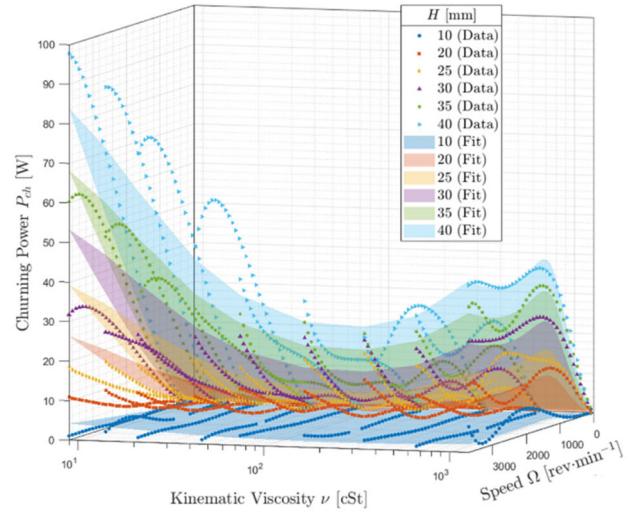


Figure 11. Predicted and measured churning losses against kinematic viscosity and speed for each immersion depth.

those of the unmodified model. This underprediction is understandable as the prediction using the modification will always be less than that of the unmodified model for non-zero rotational speeds, as the constants in Eq. [11] are unchanged from Eq. [10]. This discrepancy can be reduced by adjustment of these constants. In the tests with higher viscosity oils shown in Fig. 12c, 12d, and 12e, the unmodified model significantly overpredicts losses except at low speeds (below approximately 400, 700, and 1000 $\text{rev} \cdot \text{min}^{-1}$ in the cases of Oils 5, 7, and 9, respectively). In these cases, the reduction in effective immersion depth is much more pronounced, resulting in significantly reduced losses. In these three examples, the errors in loss predictions exceed 100% at just 2000 $\text{rev} \cdot \text{min}^{-1}$. In contrast, the modified model can predict this divergence from the simple power law relationship with speed with comparative accuracy. This shows the importance of considering the effective immersion depth when predicting gear churning losses.

The modified model showed good agreement with the experimental data, with a coefficient of determination (R^2) of 0.86 and a root mean squared error of 6.0 W across all the conditions tested. The model predictions for all the tested conditions are compared to their corresponding experimental data points in Fig. 13. It is possible to obtain a closer fit to the experimental data (with $R^2 \approx 0.93$) by using regression to adjust the constants in Eq. [11] relating to the immersion depth, Reynolds number, and Froude number. However, we reiterate that we have limited the scope of this article to a modification to an existing model to avoid overfitting to the geometries tested here.

Discussion

The results presented in this article show a complex, highly nonmonotonic relationship between oil viscosity and gear churning torque. In Fig. 6, we observe that for a high-viscosity oil, there is a local maximum in churning torque at relatively low speed followed by a plateau. In contrast, with a low-viscosity oil, there is a more gradual increase in

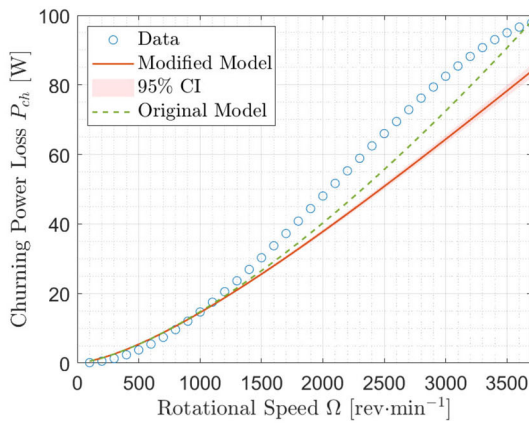
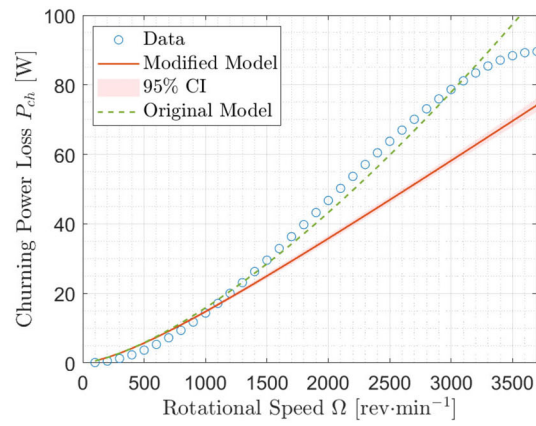
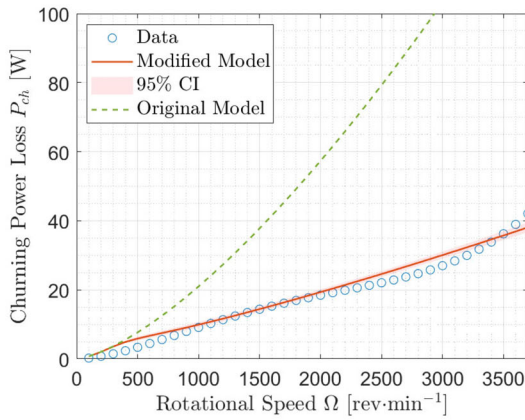
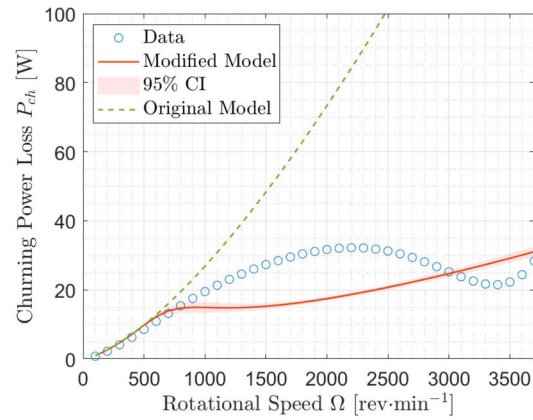
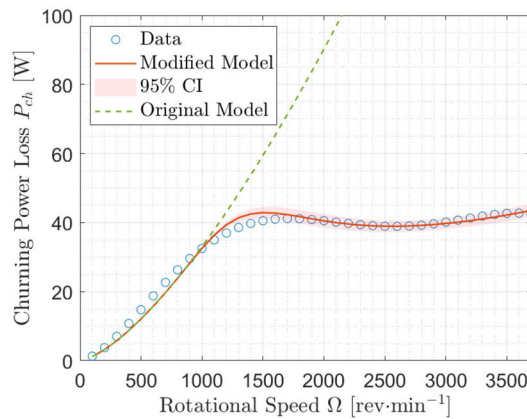

(a) Oil 1

(b) Oil 3

(c) Oil 5

(d) Oil 7

(e) Oil 9

Figure 12. Measured churning power losses with oil level $H=40$ mm, against speed compared to predictions using the new model and the model from reference (13), with 95% CIs shown.

churning torque with speed, with a local maximum at a greater speed than is observed with the high-viscosity oil. It may be the case that this is the same trend as for high viscosity but shifted to a higher speed. To illustrate this, the churning torque data shown in Fig. 6 have been replotted against the Reynolds number in Fig. 14, where the described trend is apparent. Figure 14 clearly shows a local maximum

that moves rightward towards higher Reynolds numbers as viscosity decreases. This maximum is followed by a local minimum, although for some of the lowest viscosities tested here, the existence of a local minimum is not confirmed due to the limitation in the maximum speed of the experiments. Further tests at higher speeds would be required to confirm that this minimum exists for these lower viscosities.

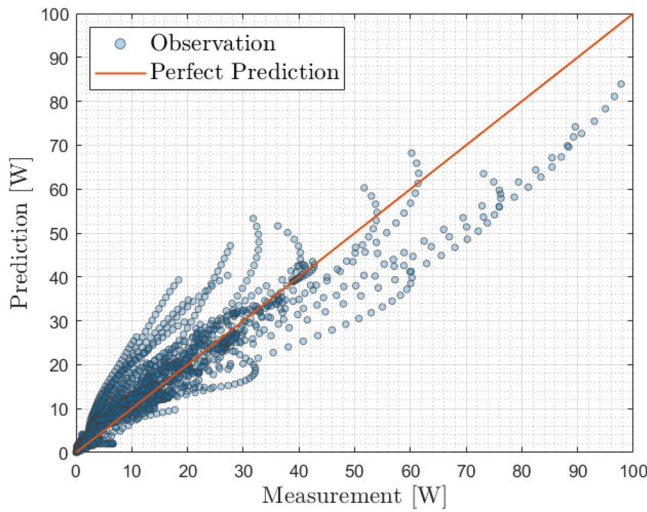


Figure 13. Model predictions versus experimental measurements.

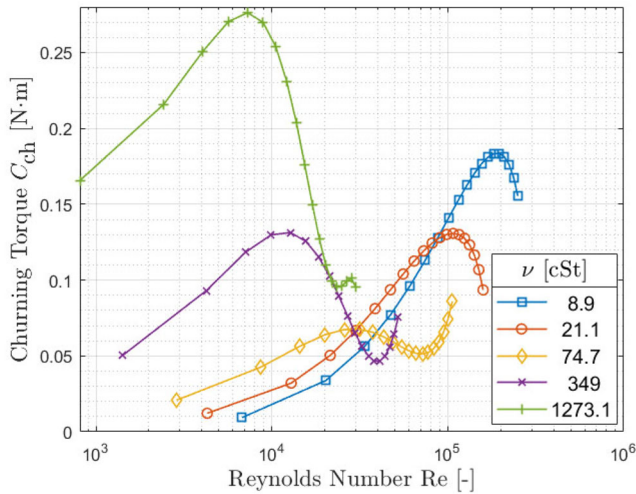


Figure 14. Churning torque data from Fig. 6 plotted against Reynolds number for a selection of viscosities.

Furthermore, if, as suggested by many existing models, a critical Reynolds number at which there is a change of regime exists, one would expect that the curves shown in Fig. 14 would overlay one another, albeit with some variation in magnitude due to differences in the lubricant density. This is clearly not the case and suggests that the Reynolds number alone is insufficient to describe the trends shown here.

An additional consequence of the observed trends is that there appears to be an optimal viscosity at which lower churning torques are observed for all speeds, as is shown in Fig. 6c. This contrasts with the conventional wisdom that continuing to reduce viscosity will lead to reduced gear churning losses and suggests that blindly reducing viscosity may be counterproductive in some instances. These results indicate that the effects of viscosity on oil surface profile need to be accounted for, as higher viscosity may lead to lower effective immersion depth at high speeds, thereby reducing churning losses. The influence of viscosity on SOSF will also have consequences beyond churning losses. While a reduction in effective immersion depth may help to

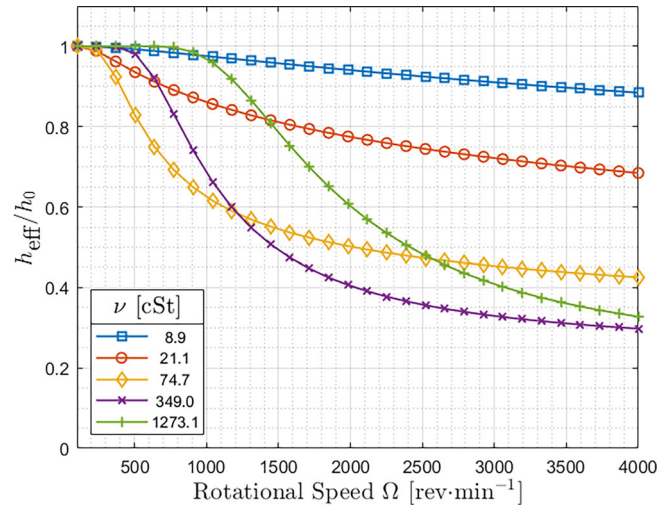


Figure 15. Effective/nominal immersion depth ratio against speed for several oil viscosities.

reduce churning losses, it may have adverse effects on other sources of power losses, as well as component reliability, as the ability of the lubricant to cool the gears will be reduced. To effectively increase gearbox efficiency without compromising reliability, this must be accounted for.

The form of Eq. [9], which attempts to capture the changes in immersion depth with speed and viscosity, describes the effects of two competing phenomena on effective immersion depth, represented by the two terms of the hyperbolic tangent function. These can be thought of as the high- and low-speed terms, respectively. As ω increases, while both terms tend toward zero, the second term does this more quickly than the first. Thus, the second term is only significant at lower speeds. In this term, the Reynolds number exponent is negative (i.e., the exponent of viscosity is positive), as at lower speeds the viscosity of the lubricant acts to prevent it from flowing away from its nominal surface profile. A higher viscosity therefore leads to an effective immersion depth closer to the nominal. In contrast, the viscosity exponent is negative in the high-speed term, as at higher speeds the centrifugal forces are sufficient to distribute the lubricant up the sides of the casing and viscous forces then act to impede flow back to the nominal oil level. As the rate of the gravitationally driven laminar flow of the oil down the sides of the casing is inversely proportional to the kinematic viscosity of the fluid (l), the effective immersion depth will have a negative correlation with viscosity. This is apparent in Fig. 9 and Fig. 10, where SOSF of the high viscosity Oil 9 is such that the effective immersion depth is more significantly reduced than is that of the low viscosity Oil 2. This agrees with the results described by Leprince et al. (4), with the low-speed term describing the flow rate of zero at the casing wall they observed at very low speeds and the effective immersion depth tending to a constant fraction of the nominal, with increasing speed describing the lack of fluid bulk motion they observed at high speed.

Example plots of effective/nominal immersion depth ratio against rotational speed are shown in Fig. 15.

Figure 15 shows how the maximum rate of decrease in effective immersion depth occurs at relatively low speeds, which is broadly in line with the observations of other authors (17, 19, 20). However, it is clear that how effective immersion depth varies with speed is strongly dependent on viscosity, something that is not accounted for by the Froude number criterion proposed by Quiban et al. (17). The criterion described by Boni et al. (19, 20) for the formation of an oil ring does account for viscosity. While making direct comparisons between their criterion and the effective immersion depth predictions described here is difficult due to the different geometries, there appears to be some agreement in the observations. For example, at the intermediate viscosities shown here the critical speed at which Boni et al. predict the formation of an oil ring is close to the speed at which the maximum rate of decrease in h_{eff}/h_0 was observed here (around $300 \text{ rev} \cdot \text{min}^{-1}$ for 75 cSt). However, there was less agreement at both very high and very low viscosities.

The proposed method to account for SOSF by considering an effective immersion depth that is dependent of the rotational speed and the oil viscosity appears to be able to closely match the experimental data, as shown in Fig. 13. While there are some discrepancies in the absolute values of losses as is to be expected, the differences in curvatures and inflexion points observed at different viscosities are fairly accurately predicted, as shown in Fig. 11 and Fig. 12, something which is not captured as well by the unmodified model.

The tests described in this article were performed with a single gear and casing geometry. As previously noted, the geometry of the system, or the presence of baffles or deflectors, will influence the effective immersion depth. Therefore, the exact expressions for effective immersion depth may differ between different geometries. However, the general trends on the effect of oil distribution on immersion depth observed here and the key conclusions of the paper, namely, that it is possible to better predict churning torque if the effective immersion depth is accounted for and that reducing viscosity will not necessarily reduce churning losses, remain valid for general casings even if the exact expression for h_{eff} may change. However, preliminary tests with a second test rig that employs a pair of meshing gears appear to show phenomena similar to the experiments described in this article. Comparisons between the results of these tests and churning loss predictions using both the modified and unmodified model suggest that predictions are improved when the effective immersion depth parameter is introduced for this setup too. The modification again allows for the nonmonotonic relationship between speed, viscosity, and churning torque to be predicted more accurately. This suggests that this simple modification to Lauster and Boos's model (13) has broader applicability than just the geometry described here and that it has practical utility in improving churning loss predictions in other gear systems.

Conclusion

In this article, the inertia rundown technique was used to experimentally assess the influence of lubricant viscosity,

rotational speed, and gear immersion depth on gear churning losses under splash lubrication. Churning torque was measured with a single gear in a cylindrical casing with nine different viscosities of group IV/PAO base stocks and for gear rotational speeds from 0 to $3700 \text{ rev} \cdot \text{min}^{-1}$.

- A clear monotonic increase in churning torque with increasing immersion depth was observed.
- The influence of viscosity on gear churning torque is complex and highly nonmonotonic. The use of higher viscosity resulted in lower churning losses in some instances, challenging the conventional wisdom that reducing viscosity reduces churning losses.
- For high-viscosity oils, churning torque increases with speed up to a certain speed; however, and somewhat counterintuitively, as speed increases further, churning torque then rapidly decreases, to reach a plateau at a relatively low torque within the speed range tested.
- In contrast, with low-viscosity oils, the gear churning torque increases with gear speed, to reach a maximum toward the highest speeds tested here.
- The local maxima and minima observed here do not appear to correspond to any specific Reynolds number.
- The trends just described were attributed to the longer time taken for the high-viscosity oil to reflow to the nominal level after being distributed up the sides of the gear case and the resulting reduction in effective immersion depth.
- There appears to be an intermediate viscosity that is optimal in terms of giving lower churning torques across the operating speed for a given geometry and operating conditions.
- An “effective immersion depth” parameter, dependent on the lubricant viscosity and angular speed of the gear, has been defined. When this parameter is incorporated into an existing empirical formula for gear churning, the nonmonotonic relationship of speed, viscosity, and churning torque observed here can be predicted with reasonable accuracy, and better than appears possible with existing empirical models.

Acknowledgements

The authors thank James Brown of Valvoline New Product Development Lab for his assistance in conducting the experiments described in this article.

Disclosure Statement

The authors declare no conflicts of interest with regards to the publication of this article.

Funding

This work was supported by the UKRI EPSRC (grant number 2293052)

ORCID

Joseph F. Shore  <http://orcid.org/0000-0003-1211-7305>
Amir Kadiric  <http://orcid.org/0000-0002-1342-3470>

References

- (1) Kolekar, A. S., Olver, A. V., Sworski, A. E., and Lockwood, F. E. (2014), “Windage and Churning Effects in Dipped Lubrication,” *J. Tribol.*, **136**(2), pp 1–10. doi:10.1115/1.4025992.
- (2) Stavvitskiy, V., Bashta, B., Nosko, P., and Tsybrii, Y. (2022), “Determination of Hydrodynamic Power Losses in a Gearing,” *Acta Mech. Autom.*, **16**(1). doi:10.2478/ama-2022-0001.
- (3) Changenet, C., and Vex, P. (2008), “Housing Influence on Churning Losses in Geared Transmissions,” *J. Mech. Des. Trans. ASME*, **130**(6), pp 0626031–0626036. doi:10.1115/1.2900714.
- (4) Leprince, G., Changenet, C., Ville, F., and Vex, P. (2012), “Investigations on Oil Flow Rates Projected on the Casing Walls by Splashed Lubricated Gears,” *Adv. Tribol.*, **2012**. doi:10.1155/2012/365414.
- (5) Höhn, B. R., Michaelis, K., and Otto, H. P. (2008), “Influence of Immersion Depth of Dip Lubricated Gears on Power Loss, Bulk Temperature and Scuffing Load Carrying Capacity,” *Int. J. Mech. Mater. Des.*, **4**(2), pp 145–156. doi:10.1007/s10999-007-9045-z.
- (6) Liu, H., et al. (2019), “Numerical Modelling of Oil Distribution and Churning Gear Power Losses of Gearboxes by Smoothed Particle Hydrodynamics,” *Proc. Inst. Mech. Eng. Part J J. Eng. Tribol.*, **233**(1), pp 74–86. doi:10.1177/1350650118760626.
- (7) Leprince, G., Changenet, C., Ville, F., Vex, P., Dufau, C., and Jarnias, F. (2011), “Influence of Aerated Lubricants on Gear Churning Losses—An Engineering Model,” *Tribol. Trans.*, **54**(6), pp 929–938. doi:10.1080/10402004.2011.597542.
- (8) Chen, S. W., and Matsumoto, S. (2016), “Influence of Relative Position of Gears and Casing Wall Shape of Gear Box on Churning Loss under Splash Lubrication Condition—Some New Ideas,” *Tribol. Trans.*, **59**(6), pp 993–1004. doi:10.1080/10402004.2015.1129568.
- (9) Changenet, C., and Vex, P. (2007), “A Model for the Prediction of Churning Losses in Geared Transmissions—Preliminary Results,” *J. Mech. Des. Trans. ASME*, **129**(1), pp 128–133. doi:10.1115/1.2403727.
- (10) Changenet, C., Leprince, G., Ville, F., and Vex, P. (2011), “A Note on Flow Regimes and Churning Loss Modeling,” *J. Mech. Des. Trans. ASME*, **133**(12), pp 1–5. doi:10.1115/1.4005330.
- (11) Boness, R. J. (1989), “Churning Losses of Discs and Gears Running Partially Submerged in Oil.” In *Proceedings of the ASME International Power Transmission and Gearing Conference*, Chicago, 1989, pp 355–359.
- (12) Terekhov, A. S. (1975), “Hydraulic Losses in Gearboxes with Oil Immersion,” *Russ. Eng. J. (English Transl. Vestn. Mashinostroeniya)*, **55**(5), pp 7–11.
- (13) Lauster, E., and Boos, M. (1983), “Zum Wärmehaushal Mechanischer Schaltgetriebe für Nutzfahrzeuge,” *VDI-Ber.*, **488**, pp 45–55.
- (14) Changenet, C., Oviedo-Marlot, X., and Vex, P. (2006), “Power Loss Predictions in Geared Transmissions Using Thermal Networks—Applications to a Six-Speed Manual Gearbox,” *Trans. ASME Downloaded*, **128**(May), pp 618–625. doi:10.1115/1.2181601.
- (15) Luke, P., and Olver, A. V. (1999), “A Study of Churning Losses in Dip-Lubricated Spur Gears,” *Proc. Inst. Mech. Eng. Part G J. Aerosp. Eng.*, **213**(5), pp 337–345. doi:10.1243/0954410991533061.
- (16) Terekhov, A. S. (1991), “Basic Problems of Heat Calculation of Gear Reducers.” In *Proceedings of Japanese Society of Mechanical Engineers International Conference on Motion and Power Transmissions*, 1991, pp 490–495.
- (17) Quiban, R., Changenet, C., Marchesse, Y., Ville, F., and Belmonte, J. (2020), “Churning Losses of Spiral Bevel Gears at High Rotational Speed,” *Proc. Inst. Mech. Eng. Part J J. Eng. Tribol.*, **234**(2). doi:10.1177/1350650119858236.
- (18) Laruelle, S., Fossier, C., Changenet, C., Ville, F., and Koechlin, S. (2017), “Experimental Investigations and Analysis on Churning Losses of Splash Lubricated Spiral Bevel Gears,” *Mech. Ind.*, **18**(4). doi:10.1051/meca/2017007.
- (19) Boni, J. B., Neuroth, A., Changenet, C., and Ville, F. (2017), “Experimental Investigations on Churning Power Losses Generated in a Planetary Gear Set,” *J. Adv. Mech. Des. Syst. Manuf.*, **11**(6), pp 1–12. doi:10.1299/jamdsm.2017jamdsm0079.
- (20) Boni, J. B., Changenet, C., Ville, F. (2021), “Analysis of Flow Regimes and Associated Sources of Dissipation in Splash Lubricated Planetary Gear Sets,” *J. Tribol.*, **143**(11). doi:10.1115/1.4051389.